

for true Ge. If so, then the high-frequency Penn-model polarizability, involving the products $M^2(E_{\vec{k},\vec{q}} - E_{\vec{k}})$, should be considerably larger than the values for Ge, whereas the low-frequency polarizability, involving the ratios $M^2/(E_{\vec{k},\vec{q}} - E_{\vec{k}})$, may

not be substantially different from the Ge case.

ACKNOWLEDGMENT

We would like to thank Professor John Walter for his help with the computer programming.

[†]Research supported in part by the National Science Foundation, under Grant No. GP 13632. Work done under the auspices of the U. S. AEC.

¹A preliminary account of the results of the present work was given by S. J. Sramek and M. L. Cohen, *Bull. Am. Phys. Soc.* **17**, 26 (1972).

²John Walter and M. L. Cohen, *Phys. Rev. B* **5**, 3101 (1972).

³D. R. Penn, *Phys. Rev.* **128**, 2093 (1962).

⁴H. Ehrenreich and M. H. Cohen, *Phys. Rev.* **115**,

786 (1959).

⁵M. L. Cohen and V. Heine, *Solid State Phys.* **24**, 37 (1971).

⁶M. L. Cohen and T. K. Bergstresser, *Phys. Rev.* **141**, 789 (1966).

⁷J. C. Phillips, *Rev. Mod. Phys.* **42**, 317 (1970).

⁸G. Srinivasan, *Phys. Rev.* **178**, 1244 (1969).

⁹John Walter and M. L. Cohen, *Phys. Rev. B* **2**, 1821 (1970).

Infrared Absorption by Coupled Surface-Phonon-Surface-Plasmon Modes in Microcrystals of CdO

K. H. Rieder, M. Ishigame,* and L. Genzel

Max-Planck-Institut für Festkörperforschung, Stuttgart, Germany

(Received 23 June 1972)

The first observation of surface-phonon-surface-plasmon coupling in small particles is reported. Thin layers of semiconducting CdO microcrystals with various free-carrier concentrations were used as samples. The coupling manifests itself in the infrared-absorption spectra through two absorption maxima corresponding to two resonances of the coupled two-oscillator system and through a pronounced absorption minimum near the transverse-optical-phonon frequency ω_T . The experimental results are discussed on the basis of a theoretical approach recently developed by Genzel and Martin. Structure in the absorption spectra near the longitudinal-optical-phonon frequency ω_L is attributed to the strong polar-optical scattering of free carriers in CdO.

I. INTRODUCTION

The phenomenon of surface-plasmon-surface-phonon coupling has met considerable theoretical interest. According to the mathematical accessibility, the problem has been studied for two situations: First, the case of infinitely extended surfaces bounding a half-space of a polar dielectric¹⁻³ and second, the case of small crystalline particles of certain shapes.^{4,5} Both cases are amenable to experimental investigations. Plasmons and phonons at extended surfaces can be studied by the prism-coupling method proposed by Otto⁶ and used already by Marschall *et al.*⁷ in studying the dispersion of surface plasmons as well as by Marschall and Fischer⁸ and also by Bryksin *et al.*⁸ in investigating surface phonons. Using the prism-coupling technique, Reshina *et al.*⁹ have observed very recently coupled surface-phonon-surface-plasmon modes at extended surfaces of *n*-type InSb. Surface phonons in small ionic crystals have been studied

extensively in the last years by infrared-absorption measurements.¹⁰⁻¹⁵ Also, surface plasmons in small metallic particles have been detected by optical methods.¹⁶⁻¹⁸ The present paper deals with the first investigation of a coupled system of surface phonons and surface plasmons in microcrystals of an ionic semiconductor by means of infrared absorption.

For an understanding of the experimental results, Sec. II gives a concise account of the theoretical approach of Genzel and Martin.⁵ Section III is devoted to a description of the experimental procedure. In Sec. IV, the experimental infrared-absorption curves are discussed on the basis of the theory.

II. THEORETICAL SURVEY

Genzel and Martin^{5,11} have developed a continuum model appropriate for describing the dielectric properties of spheres with sizes very much smaller than the wavelength of the electromagnetic radiation. They consider a medium composed of separated particles with bulk dielectric function $\epsilon(\omega)$

distributed in a material with dielectric constant ϵ_m . Defining the average electric field and the average polarization field inside the composite medium as the volume averages of the uniform fields and polarizations inside and outside the spheres, they arrive at the following expression for the dielectric response function:

$$\epsilon_{av}(\omega) = \epsilon_m \frac{\epsilon(\omega)(1+2f) + 2\epsilon_m(1-f)}{\epsilon(\omega)(1-f) + \epsilon_m(2+f)}. \quad (1)$$

Here f denotes the fraction of the total sample volume occupied by the spherical particles. The optical-absorption coefficient of the composite medium is then given by

$$K = \omega \epsilon''_{av} / c n_{av}, \quad (2)$$

where ϵ''_{av} is the imaginary part of ϵ_{av} and n_{av} is the real part of the corresponding refractive index. Thus, from the dielectric function $\epsilon(\omega)$ of the bulk material, one can calculate the dielectric properties of layers consisting of small particles. This theory was successfully used in explaining the main features of the absorption spectra of small ionic crystals.^{5,11} In Ref. 5, a discussion of the case of metallic microcrystals as well as of the situation for small particles of doped semiconductors is given. In the latter case, the dielectric function of the bulk is written as the sum of a phonon term and a free-electron Drude term:

$$\epsilon(\omega) = \epsilon_\infty + (\epsilon_D - \epsilon_\infty) + (\epsilon_L - \epsilon_\infty), \quad (3)$$

$$\epsilon_D = \epsilon_\infty \left(1 - \frac{\omega_p^2}{\omega^2 + i\omega/\tau} \right), \quad (3a)$$

$$\epsilon_L = \epsilon_\infty \frac{\omega_T^2 - \omega^2 - i\omega\gamma}{\omega_T^2 - \omega^2 - i\omega\gamma}, \quad (3b)$$

ϵ_∞ denotes the high-frequency dielectric constant, ω_T and ω_L are the transverse- and longitudinal-optical-phonon frequencies, γ is the damping function of the phonon term, and τ is the relaxation time of the electrons. The plasma frequency is given by $\omega_p = (4\pi Ne^2/m^* \epsilon_\infty)^{1/2}$, with N representing the free-electron density and m^* the effective mass of the electrons.

A discussion of Eq. (1) in connection with Eq. (3) shows in accordance to the presence of two kinds of elementary excitations, that the absorption spectrum of small crystals of a polar semiconductor exhibits two peaks due to two resonances ω_+ and ω_- of Eq. (1) with one peak lying between ω_p and ω_T , the other below ω_T . The position and the shape of the peaks depend on the electron concentration, on the damping of the system, and on the f value. For negligible damping and small f value, the following picture of the dependence of ω_+ and ω_- on the free-electron concentration is obtained: For high concentrations ($\omega_p \gg \omega_T$) the upper mode ω_+ is entirely a surface plasmon with the frequency

$$\omega_{se} = \omega_p \left(\frac{\epsilon_\infty}{\epsilon_\infty + 2\epsilon_m} \right)^{1/2} \quad (4)$$

and ω_- is a surface phonon with frequency $\omega \approx \omega_T$. At very low concentrations ($\omega_p \ll \omega_T$) the mode ω_- corresponds to the surface plasmon of Eq. (4) and the high-frequency mode ω_+ is the surface optical phonon with the Fröhlich frequency

$$\omega_F = \omega_T \left(\frac{\epsilon_0 + 2\epsilon_m}{\epsilon_\infty + 2\epsilon_m} \right)^{1/2}. \quad (5)$$

At intermediate concentrations, the two surface modes are of mixed character. A similar picture holds also for the coupled modes with large wave vectors in extended plane surfaces.^{2,3}

In addition to the two resonances, a pronounced absorption minimum close to ω_T appears, which is a striking feature of small crystal absorption for coupled systems. The position and depth of this "antiresonance" is nearly independent of the electron lifetime τ . However, its existence and shape are rather sensitive to the phonon damping γ . An experimental verification of the existence of the antiresonance constitutes a clear demonstration of surface-phonon-surface-plasmon coupling in microcrystalline systems.

III. EXPERIMENTAL

The CdO microcrystals were made by burning Cd metal in air. The specimens for the infrared transmission measurements were prepared by exposing KRS-5 or Si substrates to the smoke. Examination in an electron microscope revealed that the CdO microcrystals mainly have cubical shape and that they show a grain-size distribution similar to a Maxwellian. A mean particle size of 800 Å was determined from several electron micrographs (Fig. 1) as well as from x-ray line broadening. The electron micrographs showed also that the microcrystals are joined along edges or connected at surfaces to form treelike chains; this offers insight into the surprising fact that the particles forming a thick homogeneous layer fill space to an amount of about 3% only.

Starting with a specimen obtained in the way described above, it was possible to reduce continuously the concentration of free carriers in the crystals simply by annealing the specimens at different temperatures. The change in free-electron concentration was accompanied by a change in the color of the specimen. The bright yellow of the initial specimen changed with increasing annealing temperature to yellow red (300 °C) and red brown (550 °C) in accordance with the Burstein-Moss effect in CdO.¹⁹ Neither the mean-particle size nor the density of the film were influenced by the annealing process.

Infrared-absorption spectra were taken at room

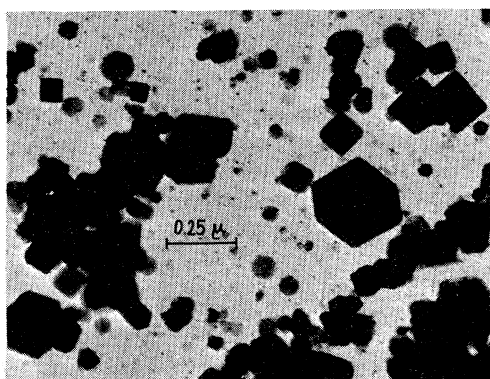


FIG. 1. Electron micrograph of CdO smoke.

temperature with the Perkin-Elmer-180 grating spectrometer in the frequency range from 4000 to 250 cm^{-1} , and with the Polytec FIR-30 Fourier spectrometer in the spectral region from 400 to 100 cm^{-1} .

IV. RESULTS AND DISCUSSION

Figure 2 shows experimental absorption curves for four different free-carrier concentrations obtained with a 30- μm layer of CdO microcrystals deposited on a Si substrate. Curve A shows the absorption spectrum of the initial specimen, the curves B, C, and D correspond to the absorption curves of the same specimen after being annealed at the temperatures 300, 460, and 550 $^{\circ}\text{C}$, respectively. The maximum temperature of 550 $^{\circ}\text{C}$ could

be reached without heat treatment damage to the Si substrates.

Before beginning the discussion of the absorption curves of Fig. 2, a few important intrinsic properties of CdO should be recapitulated. CdO is a highly degenerate ionic n -type semiconductor with NaCl structure; the free carriers stem from non-stoichiometric Cd excess. The dielectric properties of bulk CdO have been investigated by Finkenrath *et al.*²⁰⁻²²; we cite here the most important room-temperature data: $\omega_T = 262 \pm 3 \text{ cm}^{-1}$, $\omega_L = 478 \pm 25 \text{ cm}^{-1}$, $\epsilon_{\infty} = 5.4$, and $\epsilon_0 = 18.1 \pm 2.5$.

Aside from the strong absorption maximum at high frequencies, the most important structure in the CdO small crystal absorption curves of Fig. 2 appears just in the region of the transverse- and the longitudinal-optical frequencies.

Disregarding for the moment the structure near ω_L , the experimental curves exhibit just the behavior expected from theory for coupled surface-plasmon-surface-phonon systems. There is a strong absorption maximum at high frequencies, an antiresonance close to ω_T , and a second absorption maximum at frequencies just below the antiresonance. It is easily proved, that the strong absorption at high frequencies is due to the excitation of surface modes. According to Eq. (1) the resonance frequencies of the surface modes in small particles depend on the dielectric constant of the surrounding medium. In Fig. 3 experimental transmission curves of a CdO layer of about 8- μm thickness are shown. The solid curve is obtained with CdO smoke particles in air ($\epsilon_m = 1$), the broken

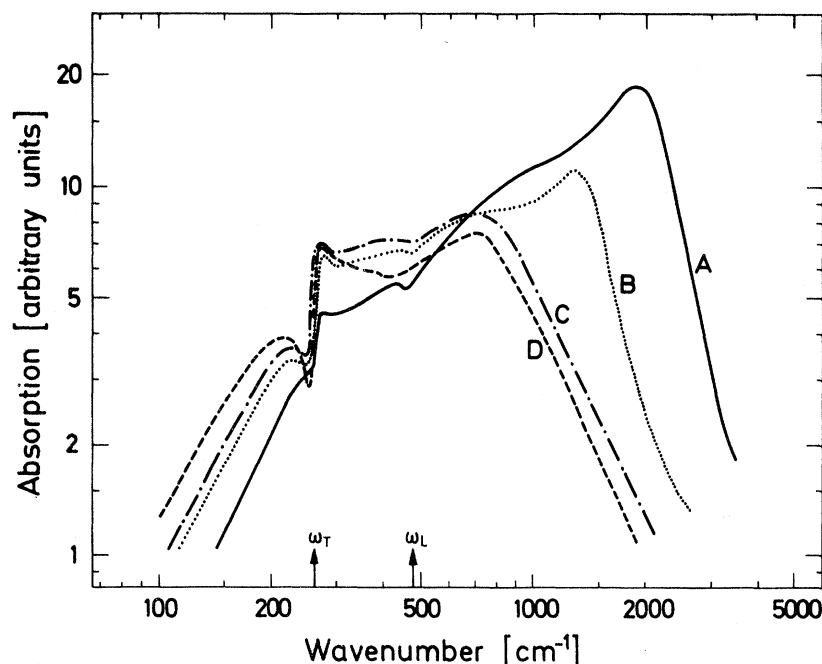


FIG. 2. Experimental absorption spectra obtained with a 30- μm layer of CdO. Curve A: CdO smoke; B: sample annealed at 300 $^{\circ}\text{C}$; C: annealing temperature 460 $^{\circ}\text{C}$; D: annealing temperature 550 $^{\circ}\text{C}$.

curve corresponds to the same sample with the microcrystals now being embedded in paraffin oil ($\epsilon_m \approx 2$). There is a large shift of the main absorption peak from 2050 to 1800 cm^{-1} ; the structure at ω_L and the peak at 270 cm^{-1} remain unaffected. Using Eq. (4), both the surface-mode frequencies in air and paraffin oil yield, in good agreement, a plasma frequency ω_p of 2400 cm^{-1} .

From the positions of the absorption maxima of curves A and B in Fig. 2, plasma frequencies of 2200 and 1550 cm^{-1} , respectively, are derived. The high-frequency absorption maxima in curves C and D of Fig. 2, however, have to be discussed below in connection with polar-optical scattering in CdO.

Contrary to the absorption curves obtained with annealed CdO samples, in the case of unannealed samples, there is no pronounced absorption minimum near ω_T due to the antiresonance characteristic for a coupled system. Only a kink near ω_T is observed. One can understand this behavior qualitatively as follows: The effect of annealing consists in a reduction of the number of defects, which are mainly Cd donors. Thus after annealing, the plasma frequency should be shifted to smaller values, and the damping of the phonons and plasmons should become smaller. Such a behavior has already been discussed for bulk CdO by Finkenrath *et al.*^{20,21} We can conclude from our experimental data that the antiresonance, which is very sensitive to the phonon damping, is suppressed by a large phonon-damping constant in the case of the unannealed CdO samples. With decreasing electron density, the number of defects is decreased and the phonon-damping constant becomes smaller, giving rise to

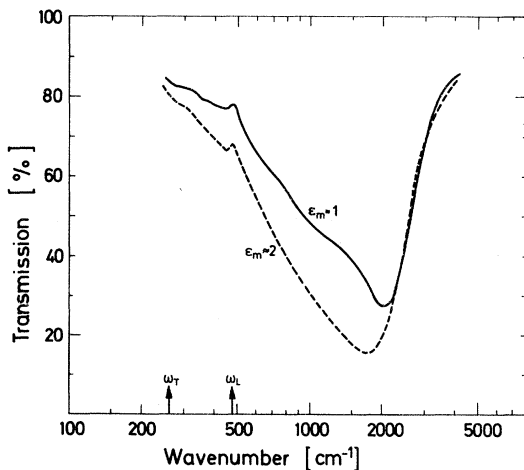


FIG. 3. Experimental transmission spectra obtained with a 8- μm layer of CdO. Solid curve: CdO smoke in air ($\epsilon_m = 1$). Broken curve: CdO smoke in paraffin oil ($\epsilon_m \approx 2$).

a pronounced antiresonance near ω_T , as found in the curves B, C, and D of Fig. 2. These results demonstrate very clearly the coupling of surface plasmons and surface phonons in microcrystalline systems.

However, in order to understand the behavior of the experimental absorption curves in more detail, the origin of the structure near ω_L must be discussed. The structure is not affected by the dielectric constant of the surrounding medium; the most striking fact is, however, that it appears just at ω_L .

It has already been pointed out by Finkenrath *et al.*²² that due to a polaron-coupling constant of $\alpha = 1.02$ ²³ in CdO, it is necessary for the description of the optical properties of CdO to account for the scattering of the free carriers on optical vibrations. The interaction of free carriers with polar-optical vibrations has been treated in several theoretical publications.²⁴⁻²⁷ Gurevich *et al.*²⁴ have given the following expression for the imaginary part of the dielectric constant of a degenerate semiconductor:

$$\epsilon_G''(\omega) = \frac{4\pi}{(3\pi^2)^{1/3}} \frac{e^4}{\hbar^2} \left(\frac{1}{\epsilon_\infty} - \frac{1}{\epsilon_0} \right) N^{2/3} \frac{\omega_T}{\omega^3} \left(1 - \frac{\omega_L}{\omega} \right). \quad (6)$$

Although this formula is derived for the conditions $\hbar\omega_L \gg kT$ and $(\hbar\omega - \hbar\omega_L) \gg kT$, it was successfully applied by Finkenrath *et al.*²² in fitting absorption spectra of bulk CdO at 300 °K. Therefore, we adopt here a similar procedure and assume the imaginary part of the dielectric function to be composed of a lattice part ϵ_L'' , the Gurevich part ϵ_G'' accounting for polar scattering and a Drude part ϵ_D'' comprising all other scattering processes:

$$\epsilon''(\omega) = \epsilon_L'' + \epsilon_G'' + \epsilon_D''. \quad (7)$$

The expressions for ϵ_L'' and ϵ_D'' are those from Eqs. (3a) and (3b); we have applied Kramers-Kronig relations to Eq. (7) to obtain the real part of the total dielectric function. By inserting Eq. (7) into Eq. (1), and by evaluating Eq. (2), absorption spectra of small CdO particles were calculated. In Figs. 4 and 5, examples of the numerical results are shown which correspond to experimental curves of Fig. 2.

Figure 4 shows calculated absorption spectra for a plasma frequency ω_p of 2200 cm^{-1} for different values of $\tau\omega_T$ and γ/ω_T . Curves 1 and 2 are obtained with the values $\tau\omega_T = 0.06$ and $\gamma/\omega_T = 0.1$, whereas curve 1 is calculated with the full dielectric function, Eq. (6), in curve 2 the Gurevich contribution has been omitted. A comparison of both curves proves the drastic difference in the region near ω_L obtained by the inclusion of polar scattering. Curve 1 exhibits a behavior very similar to the experimental curve A in Fig. 2, and curve 2 shows no structure near ω_L . However, curve 3 shows that in order to fit other parts of the

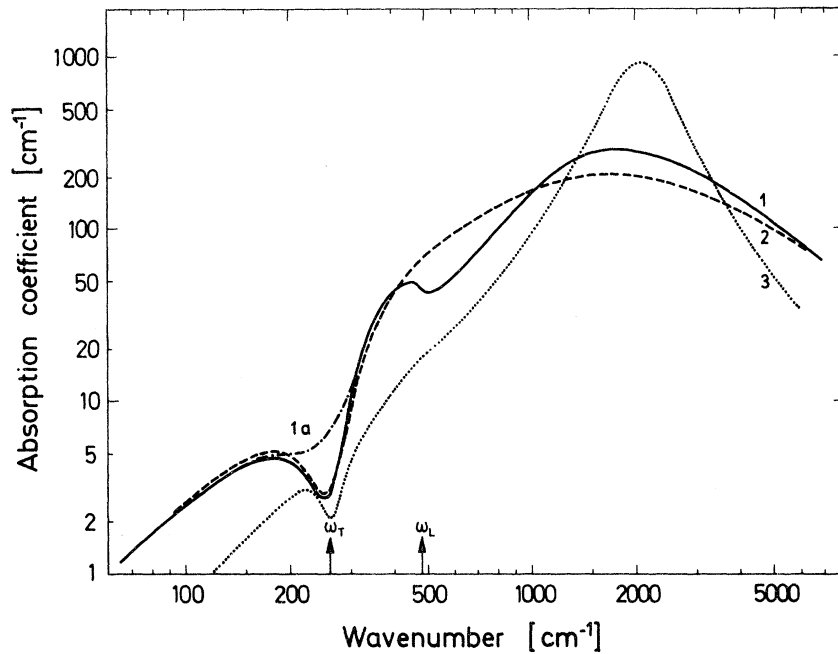


FIG. 4. Calculated absorption curves of microcrystalline CdO for $\omega_p = 2200 \text{ cm}^{-1}$. Curve 1: $\tau\omega_T = 0.06$; $\gamma/\omega_T = 0.1$. Curve 1a: $\tau\omega_T = 0.06$; $\gamma/\omega_T = 0.3$. Curve 2: Same as 1, without polar-scattering term. Curve 3: $\tau\omega_T = 0.25$; $\gamma/\omega_T = 0.1$.

experimental curve A, other damping parameters have to be used. In curve 3 the value $\tau\omega_T = 0.25$ is chosen to fit the slope of the high-frequency side of the absorption maximum; in this case the structure at ω_L is hardly visible. Curve 1 also demonstrates the drastic influence of the phonon damping on the antiresonance: whereas a value of $\gamma/\omega_T = 0.1$ produces a pronounced minimum near ω_T , the

value $\gamma/\omega_T = 0.3$ yields only a shoulder in the same region; these results illustrate the above discussion on the appearance of the antiresonance in the different experimental curves.

Figure 5 shows computed absorption spectra corresponding approximately to curve C of Fig. 2. The computed curves, obtained for a plasma frequency of 750 cm^{-1} , show that the inclusion of the

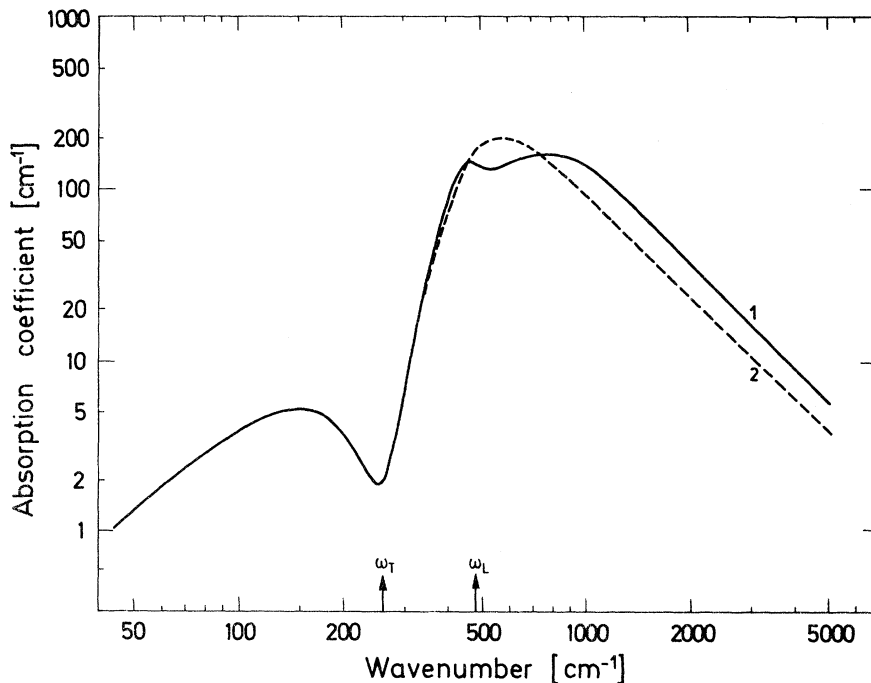


FIG. 5. Calculated absorption curves for microcrystalline CdO. Curve 1: $\omega_p = 750 \text{ cm}^{-1}$; $\tau\omega_T = 0.25$; $\gamma/\omega_T = 0.06$. Curve 2: Same as 1, without polar-scattering term.

Gurevich term into the dielectric function of CdO gives rise to a two-peak structure of the absorption curves in the frequency range near and above ω_L . It follows from Eq. (7) that the absorption maximum due to the Gurevich part should appear at $3\omega_L/2$. The calculated curve 1 of Fig. 5 as well as the experimental spectra C and D of Fig. 2 show absorption maxima very near this value. It is therefore not possible to calculate, using Eq. (4), the plasma frequencies of samples C and D from the position of the high-frequency peaks. However, we can conclude from the decrease of the absorption maximum, as well as from the decrease of the low-frequency peak and the sharpening of the antiresonance, that curve D belongs to a smaller electron concentration than curve C.

It should be mentioned at this point, that the γ values used in the calculation of the curves of Figs. 3 and 4 are greater than the γ values for similar electron concentrations given by Finkenrath²¹ for bulk CdO, whereas the τ values in our calculations had to be chosen smaller than those cited by Finkenrath.²⁰ This may indicate that both the damping of the phonons and the electrons is stronger in the microcrystals than in the bulk. A similar conclusion has been drawn for the surface phonons of MgO.¹¹

The above discussions show, that we can understand almost all features of the experimental curves on the basis of the theory⁵ if we account for the large polar scattering in CdO. A few facts, however, remain unexplained and at the present stage it is only possible to speculate about the reasons for these deviations. First, in all experimental absorption spectra, there appears a peak at 270 cm^{-1} , which does not show up in any of the calculated curves. Second, there are large discrepancies between the calculated and the measured values of the absorption coefficients: The experimental absorption coefficients extend over one order of magnitude, whereas the calculated absorption coefficients span a region of about two orders of magnitude. In connection with the latter fact, one has also to consider a frequency-dependent electron-relaxation time in the Drude term of Eq. (7) in order to be able to fit different parts of the experimental curves. Of course, instead of including the Gurevich term in an *a priori* way into the calculations of the absorption coefficients, we could have adopted the opposite way of deriving the ω dependence of $1/\tau$ from the experimental curves in analogy to the procedure of Selders *et al.*²⁸ Allowing for a ω dependent $1/\tau$ in the Drude part of Eq. (3), these authors constructed an experimental electron-damping function from reflection and transmission data of doped bulk Te and found agreement with the conclusions of Gurevich *et al.*,²⁴ whereas in the bulk the scattering of electrons is caused mainly by

longitudinal-optical phonons; in microcrystals there exist also other vibrational modes possessing inner Coulomb fields through which they can interact with electrons. Therefore, an experimentally derived ω dependence of $1/\tau$ could yield valuable information about the interaction of free carriers with vibrational modes in microcrystalline systems.

However, at the present moment it seems not to be justified to use such a procedure, because the following experimental circumstances do not meet the assumptions of the theory and therefore affect the absorption spectra in an unknown way. First, theory assumes spherical particles, whereas the microcrystals of the CdO sample are mainly of cube shape. Further, the CdO microcrystals are connected to form chains and clusters. Both facts may give rise to modified expressions for the polarization fields and therefore for the average dielectric function Eq. (1), thus producing different absorption spectra of the microcrystals. It has already been pointed out,¹¹ that the absorption spectra of $0.2\text{-}\mu\text{m}$ cubes of MgO in contrast to the theory always exhibit an absorption peak at ω_T , which should not occur for microcrystalline samples. It is therefore possible that in the case of the CdO particles a similar "bulk" absorption adds to the absorption spectra and thus gives rise to the not understood peak at 270 cm^{-1} . Since the theory⁵ is valid only for crystals very much smaller than the wavelengths of the absorbed light, the additional absorption could perhaps originate from the fraction of large particles in the CdO samples. Ruppin⁴ has calculated on the basis of Mie's theory²⁹ the absorption spectra of small spheres of polar semiconductors with diameters of about $1\text{ }\mu\text{m}$ and finds a sharp absorption peak near ω_T . However, from the results of Ruppin, it is hard to imagine that such a contribution from a small percentage of large particles can provide the one order-of-magnitude difference between the absorption coefficients of theory and experiment without hiding the antiresonance completely.

Finally, the differences in the positions of the absorption maxima of different CdO-smoke samples (see Figs. 2 and 3), would suggest that the microcrystals do not have uniform electron concentration. However, a calculation on the basis of Eqs. (7) and (1) proved that also a ω_p distribution cannot account for the discrepancy between the theoretical and experimental absorption coefficients.

Despite the remaining differences between theoretical and experimental absorption curves, we can conclude that a continuum theory, transferring simply the bulk dielectric properties of a polar semiconductor to microcrystals, can account for the interaction of coupled surface-plasmon-surface-phonon modes with light allowing one to draw qualitative conclusions about the damping of the excita-

tions in finite crystalline systems.

ACKNOWLEDGMENTS

The authors wish to express their thanks to Dr.

T. P. Martin for many valuable discussions and to Professor R. J. Bell for his interest and experimental support.

*On leave from the Research Institute for Scientific Measurements, Tohoku University, Sendai, Japan.

¹M. I. Kheifets, *Fiz. Tverd. Tela* **7**, 3485 (1965) [*Sov. Phys. Solid State* **7**, 2816 (1966)].

²K. W. Chiu and J. J. Quinn, *Phys. Letters* **35A**, 469 (1971).

³R. F. Wallis and J. J. Brion, *Solid State Commun.* **9**, 2099 (1971).

⁴R. Ruppin, *J. Phys. Chem. Solids* **30**, 2349 (1969).

⁵L. Genzel and T. P. Martin, *Surface Sci.* (to be published).

⁶A. Otto, *Z. Physik* **216**, 398 (1968).

⁷N. Marschall, B. Fischer, and H. J. Queisser, *Phys. Rev. Letters* **27**, 95 (1971).

⁸N. Marschall and B. Fischer, *Phys. Rev. Letters* **28**, 811 (1972); V. V. Bryksin, Yu. M. Gerbshtein, and D. N. Mirlin, *Fiz. Tverd. Tela* **13**, 2125 (1971) [*Sov. Phys. Solid State* **13**, 1779 (1972)].

⁹I. I. Reshina, Yu. M. Gerbshtein, and D. N. Mirlin, *Fiz. Tverd. Tela* **14**, 1280 (1972).

¹⁰For a recent review, see R. Ruppin and R. Englman, *Rept. Progr. Phys.* **33**, 149 (1970).

¹¹L. Genzel and T. P. Martin, *Phys. Status Solidi (b)* **51**, 91 (1972).

¹²M. I. Abaev, V. N. Bogomolov, V. V. Bryksin, and N. A. Klushin, *Fiz. Tverd. Tela* **13**, 1578 (1971) [*Sov. Phys. Solid State* **13**, 1323 (1971)].

¹³V. V. Bryksin, Yu. M. Gerbshtein, and D. N. Mirlin, *Fiz. Tverd. Tela* **13**, 1603 (1971) [*Sov. Phys. Solid State* **13**, 1342 (1971)].

¹⁴J. T. Luxon, D. J. Montgomery, and R. Summitt, *Phys. Rev.* **188**, 1345 (1969).

¹⁵T. P. Martin, *Phys. Rev.* **177**, 1349 (1969); *Phys. Rev. B* **1**, 3480 (1970).

¹⁶R. H. Doremus, *J. Chem. Phys.* **40**, 2389 (1964); **42**, 414 (1965).

¹⁷C. J. Duthler, S. E. Johnson, and H. P. Broida, *Phys. Rev. Letters* **26**, 1236 (1971).

¹⁸U. Kreibitz and P. Zacharias, *Z. Physik* **231**, 128 (1970).

¹⁹V. K. Miloslavskii and O. I. Shklyarevskii, *Fiz. Tekh. Poluprov.* **5**, 926 (1971) [*Sov. Phys. Semicond.* **5**, 815 (1971)].

²⁰H. Finkenrath and M. von Ortenberg, *Z. Angew. Phys.* **23**, 323 (1967).

²¹H. Finkenrath and N. Uhle, *Solid State Commun.* **5**, 875 (1967).

²²H. Finkenrath, N. Uhle, and W. Waidelich, *Solid State Commun.* **7**, 11 (1969).

²³We have obtained the value $\alpha = 1.02$ by using the value of $m^*/m_e = 0.27$ given in Ref. 13 instead of $m^*/m_e = 0.14$ as used by Finkenrath (Ref. 20).

²⁴V. L. Gurevich, I. G. Lang, and Yu. A. Firsov, *Fiz. Tverd. Tela* **4**, 1252 (1962) [*Sov. Phys. Solid State* **4**, 918 (1962)].

²⁵E. Kartheuser, R. Evrard, and J. Devreese, *Phys. Rev. Letters* **22**, 94 (1969).

²⁶J. Devreese, W. Huybrechts, and L. Lemmens, *Phys. Status Solidi (b)* **48**, 77 (1971).

²⁷J. Devreese, J. De Sitter, and M. Goovaerts, *Phys. Rev. B* **5**, 2367 (1972).

²⁸M. Selders, P. Gspan, and P. Grosse, *Phys. Status Solidi (b)* **57**, 519 (1971).

²⁹G. Mie, *Ann. Physik* **25**, 377 (1908).

Electrostatic Edge Modes in a Dielectric Wedge

L. Dobrzynski* and A. A. Maradudin†

Department of Physics, University of California, Irvine, California 92664

(Received 24 April 1972)

The dispersion relations are obtained for electrostatic modes localized in the vicinity of the edge of a dielectric wedge formed by the intersection of two semi-infinite planes making an interior angle of 2α . The dielectric constant of the medium is assumed to be isotropic. The resulting modes can be classified as even or odd under reflection in the plane bisecting the wedge. Their frequencies are functions of one continuously varying quantum number. The general results obtained are specialized to yield the dispersion relations for edge optical modes and edge plasmons. Properties of dielectric edge modes are compared and contrasted with corresponding properties of surface modes.

It is well known¹ that at the plane interface between a dielectric medium and the vacuum it is possible for electromagnetic excitations to exist which, while wavelike in directions parallel to the interface, decay exponentially in amplitude with

increasing distance from the interface both into the medium and into the vacuum. Such surface excitations have recently been the objects of experimental study.²

In this paper we investigate a related problem,

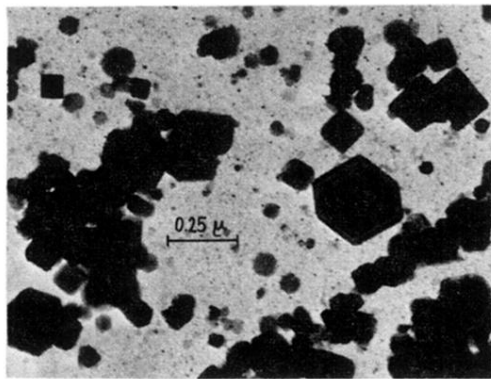


FIG. 1. Electron micrograph of CdO smoke.